Dijlah Journal of Medical Sciences (DJMS) Vol. 3, No. 3, September, 2026, pp. 43-56
P-ISSN: 3078-3178, E-ISSN: 3078-8625, paper ID: 05

ORIGINAL ARTICLE

Targeting Drug-Resistant Cancer with Copper (II) Schiff Base Complexes

Dhuha Khudhair Rashid AL Musawi*
Al Fatwa Intermediate School for Boys, Directorate of Education in Al Rusafa First, Baghdad, Iraq

Article Info

Article history:

Received June, 15, 2026
Revised July, 10, 2026
Accepted July, 15, 2026

Keywords:

Schiff Base Complexes of Copper Binary,
Anti-Cancer Activity,
Regulation of Oxidative Stress

ABSTRACT

Metal-based drugs hold potential as a means to circumvent drug resistance in cancer. In this work ،a number of new copper (II) Schiff base complexes with tridentate phenim ligand were prepared and identified by FT-IR ،UV-Vis and elemental (CHN) analysis. The spectroscopy indicated that the ligand coordinates to the Cu (II) ion through the azomethine and pyridine nitrogen atoms ،resulting in stabler complexes with specific geometries. CuSB-1 [Cu (phenim) Cl_2] was found to be the most active of the compounds synthesized. Cytotoxicity assays showed good anti-proliferative activity against MCF-7, PC3 and HEK-293 cell lines, with significantly lower IC_{50} values than other complexes and Cisplatin. CuSB-1 was found to effectively interact with DNA, likely via non-covalent binding (intercalation). In vivo studies on a rat breast tumor model demonstrated that CuSB-1 efficiently inhibited tumor growth, lowered specific growth rate and extended the tumor doubling time, surpassing cisplatin. Biochemical and histopathological studies showed increased apoptosis induction and decreased tumor proliferation. Moreover ،antioxidant enzyme analysis suggested that CuSB-1 alters the redox balance by reducing the activity of catalase and glutathione peroxidase ،and increasing the activity of glutathione reductase ،thereby increasing the level of oxidative stress. As a whole, the anticancer effects of CuSB-1 are mediated through a multi-pronged mechanism of action ،which includes DNA binding, induction of oxidative stress and activation of apoptosis. The results suggest CuSB-1 could be a lead compound in the development of novel copper-based antitumor drugs.

Corresponding Author:

* Dhuha Khudhair Rashid AL-Musawi
Al Fatwa Intermediate School for Boys, Directorate of Education in Al Rusafa First, Baghdad, Iraq
Email: dhuhaa267@gmail.com

1- INTRODUCTION

The accidental discovery of Cisplatin by Barnett Rosenberg *et al.*, 1969 [1] marked the start of the evolution of metal-based drugs towards new chemotherapeutic agents. These drugs are usually metal complexes that bind to nucleobases in DNA [2], or hydrolytically or oxidatively cleave the DNA molecule [3،4]. This damage results in the cells' apoptosis، either from irreparable DNA damage or by the blockade of cell cycle transcription factors. First-generation metallodrug، cisplatin، binds to DNA at the N7 position of guanine to form platinum–DNA adducts، thereby triggering DNA damage response proteins. These proteins block the activity of cyclin-dependent kinases (CDKs)، and induce apoptosis through the p53 pathway [5،6]. But the major drawbacks of cisplatin are drug resistance and its high toxicity [7،8]. This has prompted the need for ligand modification and alternative، more

biocompatible metal complexes that can bind to DNA in a physiological environment. A number of first-row transition metals are essential parts of metalloproteins with various biological functions. Copper is of particular interest because it is found in enzymes such as Zn-Cu superoxide dismutase [9], tyrosinase [10]، dopamine β-hydroxylase [11], cytochrome c oxidase [12] and blue copper proteins [13]. Copper complexes have been widely investigated due to their biologically relevant redox chemistry and high binding affinity towards nucleobases [14،15]. These complexes are known to possess oxidative، hydrolytic and photolytic nuclease activities [16]. In addition، bis (salicylate) copper (II) complexes have been reported to have synergistic effects with antioxidant agents such as curcumin-derived diketimines, and exhibit cytotoxicity and antivirality [17]. Copper complexes with glycine have also been found to reverse drug resistance in T-cell acute lymphoblastic leukemia (CEM) cells [18]. Most recently، Schiff base copper complexes containing quinoline have been found to be proteasome inhibitors in prostate cancer [19]. Taken together، these studies suggest that copper complexes are able to affect both DNA and protein function، which can be used to our advantage.

The complexes studied in this work are mononuclear copper complexes with a Schiff base ligand having two pyridine and one azomethine (imine) nitrogen donors، and other various monodentate ligands (Figure 1). First، a number of copper complexes were tested for their cytotoxicity (MTT assay). The complex [Cu(phenim)Cl2] (CuSB-1), with the smallest IC_{50} value، was chosen for further investigations. The MCF-7 cell line was initially used to test its anticancer activity before performing in vitro experiments on tumor-bearing rats.

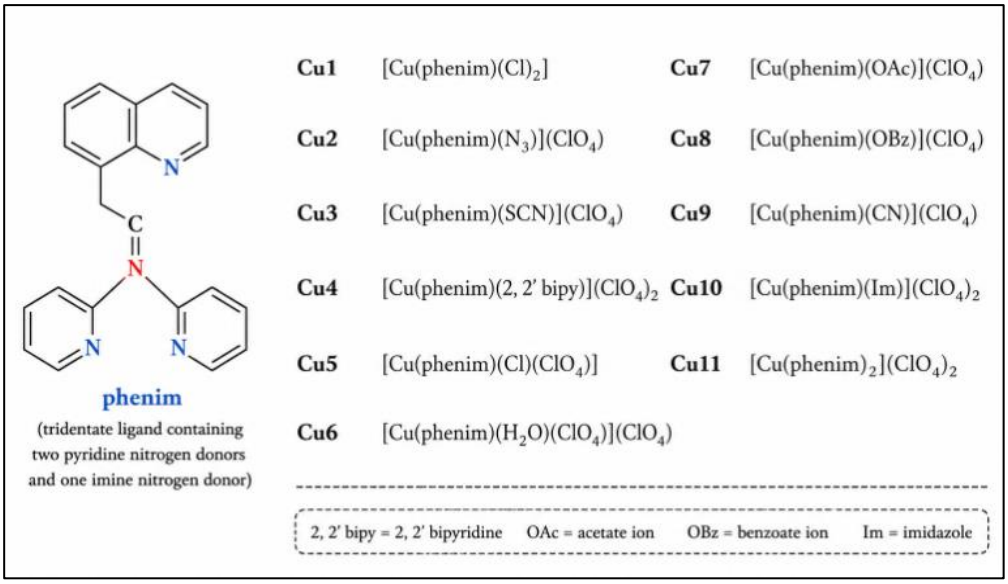

Fig (1): Basic structure of the family of copper complexes

The emergence of multidrug resistance (MDR) in cancer cells remains a major obstacle to effective chemotherapy, leading to therapeutic failure and poor clinical outcomes. This challenge necessitates the development of novel anticancer agents capable of circumventing resistance mechanisms. Copper (II) Schiff base complexes have attracted significant attention as promising candidates due to their versatile coordination chemistry and potent biological activity. This study synthesizes and characterizes a series of copper (II) Schiff base complexes to assess their anticancer potential. Particular attention is given to CuSB-1 [Cu(phenim)Cl_2], identified as the most active complex, and to determining how it acts against drug-resistant cancer cells. The investigation examines its cytotoxicity and DNA-binding ability, along with its in vivo antitumor efficacy and capacity to induce apoptosis by modulating oxidative stress.

2- MATERIALS AND METHODS

2.1 Chemicals and Reagents

The human breast cancer (MCF-7)، prostate cancer (PC3), and human embryonic kidney (HEK-293) cell lines were procurement from a certified cell line bank. Culture media (Dulbecco's Modified Eagle Medium (DMEM)، DMEM-F12), fetal bovine serum (FBS)، and antibiotics (penicillin and streptomycin) were obtained from common vendors. Chemicals، such as MTT (3-(4،5-dimethyl-2-thiazolyl)-2،5-diphenyl-2H-tetrazolium bromide),

dimethyl sulfoxide (DMSO)، agarose، and buffers of high purity were sourced from established vendors. Cisplatin was employed as a positive drug. N-Methyl-N-nitrosourea (MNU)، BCA protein estimation kits and antioxidant enzyme assay kits were obtained from Sigma-Aldrich. All the solutions were prepared in double-distilled water.

2.2 Preparation of Schiff Base Ligand (phenim)

The Schiff base ligand (phenim) was prepared by the reaction of a heteroaromatic aldehyde with a pyridine amine in ethanol and refluxed for 3-5 h. After cooling to room temperature، the solid was filtered، washed with cold ethanol، and dried in vacuo. The formation of the azomethine (C=N) bond was confirmed by spectroscopy [20].

2.3 Copper (II) Complex (CuSB-1)

The copper (II) complex [Cu(phenim)Cl2] (CuSB-1) was prepared by refluxing the ligand with $CuCl_2 \cdot 2H_2O$ in ethanol for 2-3 h. The copper (II) complex was isolated by filtration، washed and dried in vacuo. Other members of the series were synthesised similarly، using different monodentate ligands (e.g. Cl-، N3-، SCN-، CN-، OAc-، OBz-، H2O) and a bis-complex، Cu $(phenim)_{22}$، was also prepared [21].

2.4 Characterization Techniques

The newly prepared compounds were analysed by FT-IR (to check coordination of the ligand through C=N stretching vibration), UV-Vis (to observe d-d and charge transfer) and elemental (CHN) analysis. These confirmed the formation of complexes and their purity.

2.5 Cell Culture

MCF-7 and HEK-293 cells were cultured in DMEM، and PC3 cells in DMEM-F12 medium، both containing 10% heat-inactivated FBS and 1% antibiotics (100 U/mL penicillin and 100 μg/mL streptomycin). The cells were cultured at 37°C in a humidified 5% CO_2 incubator.

2.6 Cytotoxicity Assay (MTT Assay)

The MTT assay was used to determine cell viability. Cells (5×10^3 per well) were cultured in 96-well plates overnight. The cells were then exposed to different concentrations (0.05-100 μM) of CuSB-1 for 24 h. Cells were incubated with MTT solution (5 mg/mL) for 4 h at 37°C. DMSO was added to dissolve formazan crystals and absorbance was read at 570 nm. Inhibition percentage was measured and IC_{50} values calculated using GraphPad Prism [22].

2.7 DNA Binding Studies

Calf thymus DNA was pre-treated with ethidium bromide، and fluorescence quenching experiments were performed. Various amounts of CuSB-1 (0-50 μM) were added and emission spectra were measured. The Stern-Volmer equation was used to determine the binding constants.

2.8 *In Vivo* Antitumor Study

Female rats were induced with breast tumors using MNU (50 mg/kg، i.v). Rats were grouped into control and experimental groups. CuSB-1 and cisplatin were given i.p. (1 mg/kg body weight twice a week for 4 weeks).

The volume was calculated as [23]:

$$V = 0.44 \times A \times B^2 \qquad (1)$$

Where A and B represent tumor diameters. Tumor growth rate and doubling time were calculated accordingly.

2.9 Histopathological Analysis

Tumor tissues were fixed in formalin، embedded in paraffin، cut into 5 μm sections and stained with hematoxylin and eosin. The mitotic and apoptotic indices were determined by counting cells microscopically.

2.10 Antioxidant Enzyme Assays

Catalase، glutathione peroxidase and glutathione reductase activities were spectrophotometrically determined in tumor tissue homogenates (nmol/mg protein/min).

2.11 Statistical Analysis

The experiments were carried out in triplicates and the results were presented as mean ± SEM. One-way ANOVA and Student's t-test were used for statistical analysis. A p-value < 0.05 was considered statistically significant.

3- RESULTS AND DISCUSSION

3.1 FT-IR Spectral Analysis

The FT-IR technique was used to verify the coordinating ability of phenim towards Cu (II) in Cu1-Cu11. The free Schiff base (phenim) ligand showed a bands at around 1625 cm^{-1}، which is a typical feature for the azomethine (C=N) stretching vibration، indicating the imine linkage. This band was observed at lower frequencies (1598-1612 cm^{-1}) in all complexes (Cu1-Cu11), suggesting coordination of the azomethine nitrogen atom to the Cu(II) center. The pyridine ring stretching bands (1480-1500 cm-1) were also shifted (5-10 cm-1) in the complexes، indicating the coordination of pyridine nitrogen atoms. The new bands observed in the low-frequency region (510-540 cm^{-1} and 420-460 cm^{-1}) were assigned to ν(Cu-N) and ν(Cu-Cl/O/N) vibrations، respectively، confirming complexation. The FT-IR spectral data of the phenim and its copper (II) complexes (Cu1-Cu11) are listed in Table 1، which reveal the involvement of azomethine and pyridine nitrogen atoms in coordination.

Table (1): FT-IR spectral data (cm^{-1}) of the phenim ligand and Cu (II) complexes (Cu1-Cu11)

Compound	ν(C=N) (azomethine)	ν(C=N) shift	Pyridine ν(C=C/C=N)	ν(Cu–N)	ν(Cu–X)*	Other characteristic bands
phenim (ligand)	1625		1485–1500			
Cu1	1608	↓17	1490	520	430 (Cl)	
Cu2	1605	↓20	1492	525	445 (N_3)	2030 (N_3^-)، 1090، 625 (ClO_4^-)
Cu3	1602	↓23	1488	530	450 (SCN)	2080 (SCN^-)، 1085، 620 (ClO_4^-)
Cu4	1600	↓25	1495	535	455 (bipy)	1095، 625 (ClO_4^-)
Cu5	1607	↓18	1491	522	435 (Cl)	1090، 622 (ClO_4^-)
Cu6	1609	↓16	1493	518	425 (H_2O)	1088، 620 (ClO_4^-)
Cu7	1604	↓21	1489	528	440 (OAc)	1550، 1410 (COO^-)، 1092، 625
Cu8	1601	↓24	1490	532	448 (OBz)	1600، 1385 (COO^-)، 1085، 622
Cu9	1598	↓27	1487	540	460 (CN)	2120 (CN^-)، 1090، 625
Cu10	1603	↓22	1492	530	450 (Im)	1093، 623 (ClO_4^-)
Cu11	1606	↓19	1494	525	—	1095، 625 (ClO_4^-)

Overall، FTIR results clearly indicate that the phenim ligand acts as a tridentate N، N، N donor، coordinating through two pyridine nitrogen atoms and one azomethine nitrogen.

3.2 UV–Visible Spectral Analysis

The UV-Vis spectral features of the complexes (Cu1-11) are outlined in Table 2، which reveal ligand-based، LMCT and d-d transitions، as expected for Cu (II) complexes.

Table (2): UV-Vis spectral data (λmax، nm) of Cu (II) complexes (Cu1-Cu11) in DMSO

Complex	π→π* (nm)	n→π* (nm)	LMCT (nm)	d–d transition (nm)	Geometry (proposed)
Cu1	268	332	402	645	Distorted square pyramidal
Cu2	272	338	410	655	Distorted octahedral
Cu3	275	342	420	670	Distorted octahedral
Cu4	270	335	408	660	Distorted octahedral
Cu5	266	330	400	640	Square pyramidal
Cu6	269	333	395	635	Octahedral
Cu7	271	336	405	650	Square pyramidal
Cu8	273	340	412	665	Distorted octahedral
Cu9	278	345	430	690	Distorted octahedral
Cu10	270	337	410	655	Distorted octahedral
Cu11	267	331	398	642	Octahedral

The λmax values of Cu1-Cu11 complexes showed minor differences based on the monodentate ligand، suggesting variations in the ligand field strength. A bathochromic shift was observed for complexes with stronger field ligands (CN^-، SCN^-), indicating stronger ligand-metal interactions.

3.3 Elemental (CHN) Analysis

CHN elemental analysis was used to verify the purity of the complexes. The observed values were found to be in close agreement with the theoretical values for all complexes (Cu1-Cu11), suggesting successful synthesis and good purity. The elemental (CHN) analysis data (Table 3) revealed calculated and experimental values in good agreement، confirming the proposed molecular formula as well as the purity of all the complexes.

Table (3): Elemental (CHN) analysis of Cu (II) complexes (Cu1-Cu11)

Complex	C (%) Calc.	C (%) Found	H (%) Calc.	H (%) Found	N (%) Calc.	N (%) Found
Cu1	52.14	51.98	3.85	3.79	10.12	10.05
Cu2	50.86	50.70	3.78	3.70	13.45	13.30
Cu3	49.76	49.60	3.62	3.55	12.45	12.30
Cu4	53.10	52.90	3.95	3.88	11.20	11.05
Cu5	51.48	51.30	3.82	3.75	10.05	9.92
Cu6	50.95	50.78	3.88	3.80	9.85	9.70
Cu7	50.21	50.05	3.90	3.82	9.88	9.76
Cu8	52.05	51.85	3.96	3.88	9.60	9.48
Cu9	48.90	48.75	3.55	3.48	11.95	11.80
Cu10	51.60	51.42	3.87	3.79	10.30	10.15
Cu11	54.32	54.10	4.12	4.05	11.65	11.50

The minimal difference (< ±0.4%) between the calculated and experimental values suggests the complexes' stoichiometric purity.

3.4 Antiproliferative Activity of CuSB-1

The comparative IC_{50} values of the copper(II) complexes (Cu1-Cu11) against MCF-7، HEK-293 and PC3 cell lines using MTT assay are shown in Table 4. The values represent mean ± SEM of three experiments. Complexes Cu1، Cu3، Cu5، Cu7 and Cu9 exhibited relatively low IC_{50} values against all the three cell lines. But CuSB-1 [Cu(phenim)Cl_2] was chosen for further studies due to two reasons:

i. Its relatively low IC_{50} values for all the tested cell lines، and
ii. Its better solubility in the experimental conditions than other complexes.

Table (4): In vitro cytotoxicity (IC_{50}، µM) of copper (II) complexes with phenim against cancer cells

Compound	IC_{50} (µM) MCF-7	IC_{50} (µM) PC3	IC_{50} (µM) HEK-293
CuSB-1 [Cu(phenim)Cl_2]	4.18 ± 0.39	6.12 ± 0.54	5.26 ± 0.41
Cu2	16.02 ± 1.08	10.75 ± 0.47	12.95 ± 2.05
Cu3	7.42 ± 0.58	13.25 ± 2.45	10.68 ± 1.29
Cu4	10.35 ± 0.31	8.52 ± 0.44	16.10 ± 1.36
Cu5	7.30 ± 0.60	7.85 ± 0.65	10.95 ± 0.40
Cu6	14.20 ± 1.70	7.85 ± 0.90	18.30 ± 3.10
Cu7	7.60 ± 0.20	5.05 ± 1.02	10.72 ± 1.55
Cu8	14.10 ± 1.20	11.05 ± 0.45	8.45 ± 1.55
Cu9	9.20 ± 0.34	5.25 ± 0.47	6.30 ± 0.48
Cu10	47.90 ± 1.20	10.20 ± 0.52	66.80 ± 5.10
Cu11	10.85 ± 0.52	10.45 ± 0.34	14.10 ± 1.85
$CuCl_2$	>100	>100	>100
phenim (ligand)	9.05 ± 0.25	95.80 ± 2.10	>100
Cisplatin	62.50 ± 3.50	78.90 ± 5.10	76.40 ± 3.20

3.5 DNA Binding Studies

The fluorescence intensity of the ethidium bromide (EB)–calf thymus DNA complex was quenched by increasing concentrations of CuSB-1 (0-50 µM) as shown in Figure 2. This is suggestive of the displacement of DNA-bound EB by CuSB-1. There was no appreciable quenching of fluorescence in the absence of DNA or EB، despite the presence of CuSB-1. In addition، there was no such effect in the presence of either the free ligand (phenim) or the copper salt ($CuCl_2$).

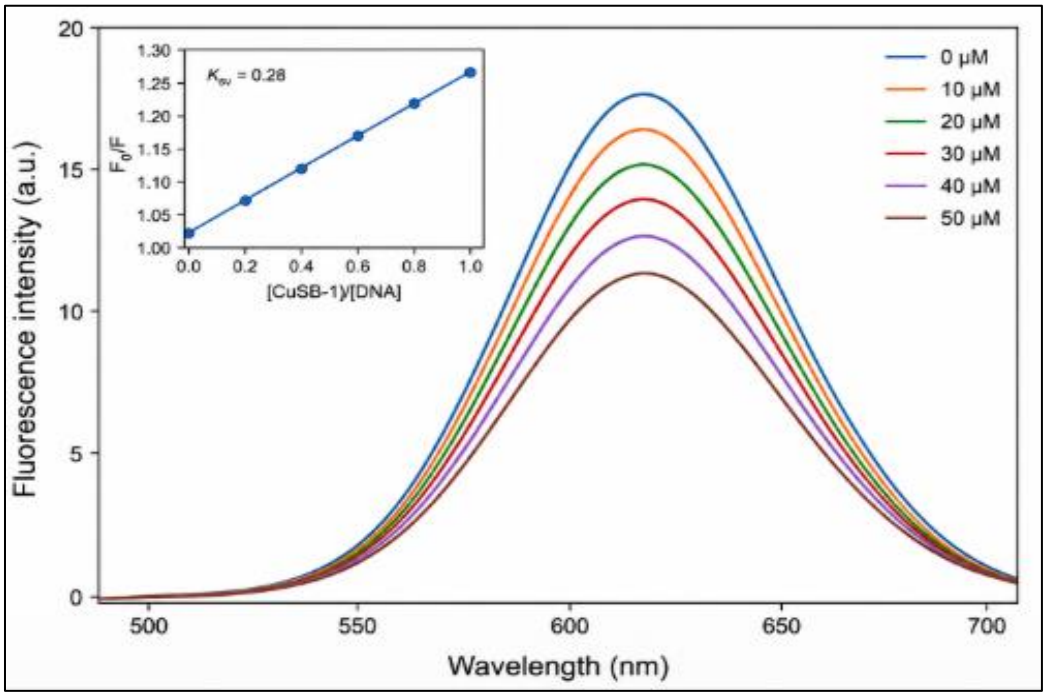

Fig (2): Fluorescence quenching of calf thymus DNA-ethidium bromide complex with increasing concentrations of CuSB-1 [Cu(phenim)Cl_2]. The inset is the Stern–Volmer plot of I_0/I (where I_0 is the fluorescence intensity in the absence of CuSB-1 and I the fluorescence intensity in the presence of CuSB-1) versus [CuSB-1]/[DNA]، showing the binding of the copper(II) complex with DNA

The Stern-Volmer quenching constant (KSV)، obtained from the linear regression of the plot، was found to be 0.28، implying that CuSB-1 has a moderate binding constant with DNA.

3.6 Antitumor Effect of CuSB-1

Following treatment with CuSB-1 [Cu(phenim)Cl_2] for one month، the specific tumor growth rate in the Group III animals decreased by ~55%، while only a ~22% decrease was seen in the Cisplatin-treated group (Group IV)، compared with no treatment tumor-bearing animals (Group II) ($p < 0.05$). Moreover، the tumor doubling time (DT) almost doubled، as observed in previous reports (Sánchez et al.، 2006) (Table 3). As shown in Figure 3، a remarkable suppression ($p < 0.05$) in the tumor growth rate was observed within two weeks of treatment with CuSB-1، which was further enhanced after four weeks ($p < 0.01$). By contrast، cisplatin only showed significant effects on tumor prevention after four weeks ($p < 0.05$).

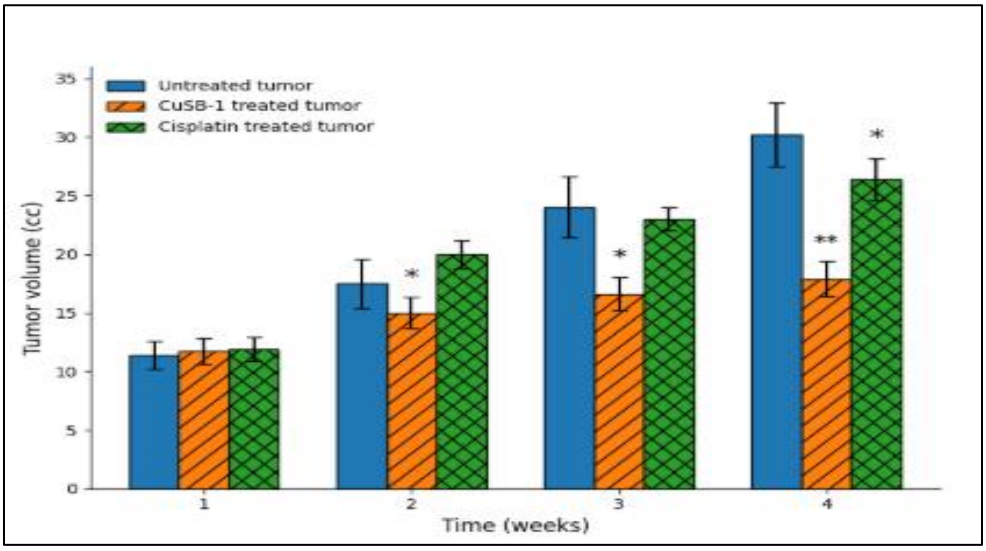

Fig (3): Tumor volume changes in tumor-bearing animals after the treatment with CuSB-1 [Cu(phenim)Cl_2] and Cisplatin over 4 weeks. Data are presented as mean ± S.E.M. (n = 11). * And ** represent statistically significant differences at $p < 0.05$ and $p < 0.01$، respectively، from the untreated tumor group at the same time intervals

The significant gain in body weight seen in untreated tumor-bearing animals - likely a consequence of growing tumors - was significantly decreased after treatment with CuSB-1 ($p < 0.01$) and cisplatin ($p < 0.05$) at four weeks، but to a greater extent with CuSB-1 (Figure 4).

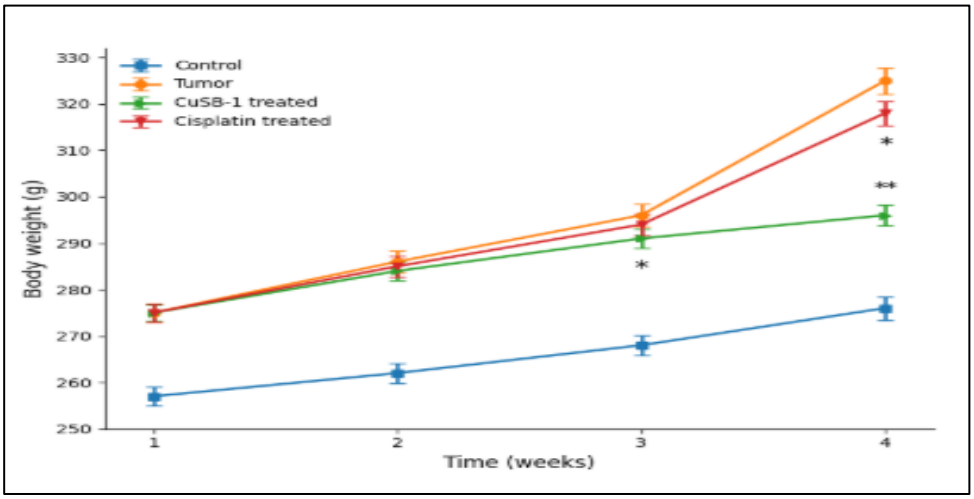

Fig (4): Body weight variations of animals during the course of treatment with CuSB-1 [Cu(phenim)Cl_2] and Cisplatin. Data represent mean ± S.E.M (n = 11 for tumor and treatment groups; n = 10 for control group). * and ** represent significant differences ($p < 0.05$ and $p < 0.01$، respectively) compared to the control group (tumor) at the same time points

In summary، these results show that، although cisplatin is very effective in vitro، it's in vivo antitumor activity was relatively weak، while CuSB-1 demonstrated stronger antitumor effects (Figures. 3، 4، and Table 5).

Table (5): Inhibition of breast tumor growth by CuSB-1 in vivo

Treatment	Initial tumor volume (cc)	Final tumor volume (cc) after 30 days	Specific growth rate	Tumor doubling time (days)
Group I (vehicle-treated، n = 10)	ND	ND	ND	ND
Group II (tumor control، n = 11)	11.4 ± 1.4	30.2 ± 2.7	0.033	21
Group III (CuSB-1 treated، n = 11)	11.7 ± 1.3	17.9 ± 1.5[a]	0.015	45
Group IV (Cisplatin treated، n = 11)	11.9 ± 1.2	26.4 ± 1.8[b]	0.025	28

3.7 Histopathological Findings

Histology studies showed that after one month of treatment with CuSB-1 [Cu(phenim)Cl_2], multiple apoptotic bodies were formed in the breast tumor tissues (Figure 5C، with higher magnification in Figure 5D، arrows). By contrast، the untreated tumor-bearing group showed a large number of proliferating ductal carcinoma cells، filling the whole microscopic field (Figure 5B). The histological analysis of the Cisplatin-treated group showed only slight changes compared to the vehicle-treated group، with a few apoptotic bodies (Figure 5E and 5F). Breast sections of control animals (Figure 5A) did not show any proliferating cells or apoptotic bodies، and showed normal tissue architecture.

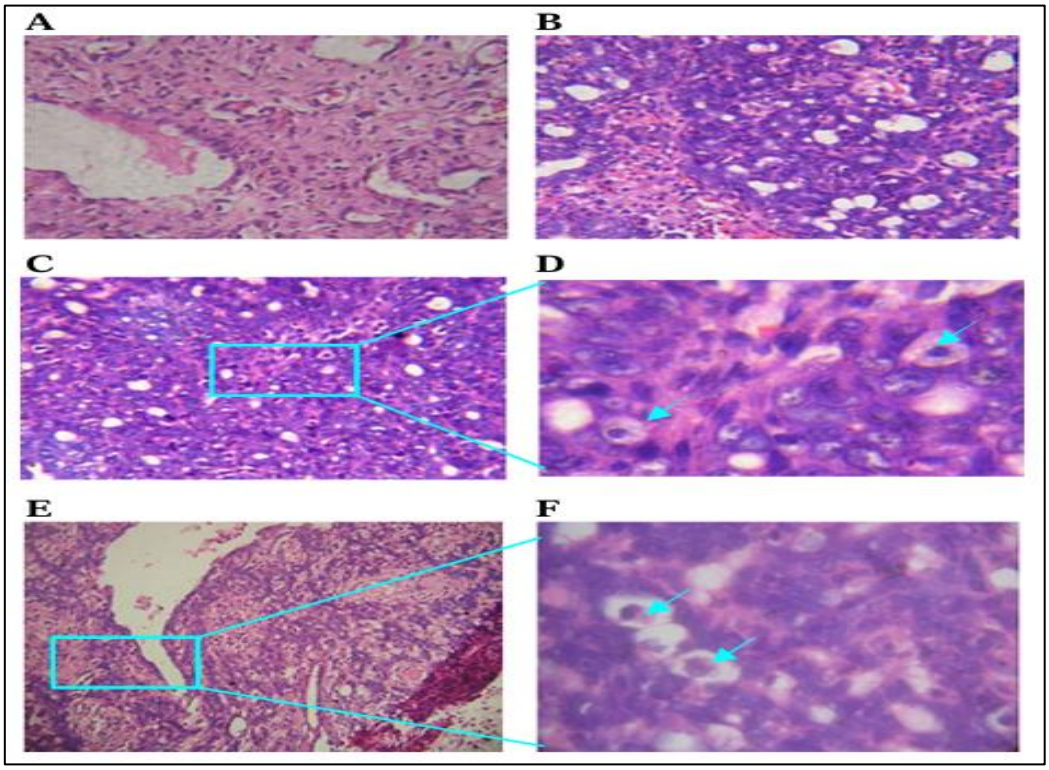

Fig (5): Hematoxylin and eosin (H&E) staining of breast tissues from various groups. (A) Control group (200×); (B) untreated tumor group (200×); (C) tumor treated with CuSB-1 [Cu(phenim)Cl_2] (200×); (D) magnified view of apoptotic cells with chromatin condensation (indicated by arrows) (400×); (E) tumor treated with Cisplatin (200×); and (F) magnified view of apoptotic cells with chromatin condensation (indicated by arrows) (400×)

As shown in Figure 6، CuSB-1 treatment resulted in a significant decrease in the mitotic index ($p < 0.05$) and a significant increase in the apoptotic index ($p < 0.01$). While cisplatin also increased the apoptotic index ($p < 0.05$)، the effect was not as significant as that observed with CuSB-1.

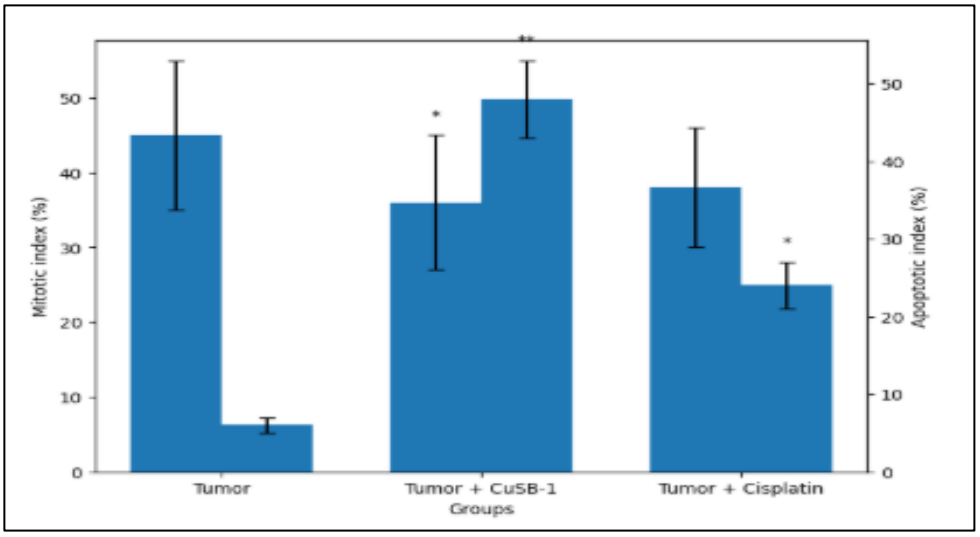

Fig (6): Mitotic index and apoptotic index in tumor tissues after treatment with CuSB-1 [Cu(phenim)Cl_2] and Cisplatin in H&E stained tissue sections. Data are expressed as mean ± S.E.M of at least 10 different fields in each group. * and ** represent significant difference at $p < 0.05$ and $p < 0.01$، respectively، from untreated tumor animals

These results are in agreement with previous reports، suggesting that CuSB-1 has a better effect than cisplatin in inducing apoptosis in tumor tissues.

3.8 Antioxidant Enzyme Analysis

We evaluated the effects of CuSB-1 [Cu(phenim)Cl_2] on tumor tissues by measuring antioxidant enzymes. Figure 7 shows that the activity of catalase and glutathione peroxidase was decreased by about 5-fold and 1.5-fold، respectively، after CuSB-1 treatment as compared to the untreated tumor group. However، the activity of glutathione reductase was significantly higher (2-fold، $p < 0.05$) in CuSB-1-treated tumor tissues compared to untreated tumor tissues.

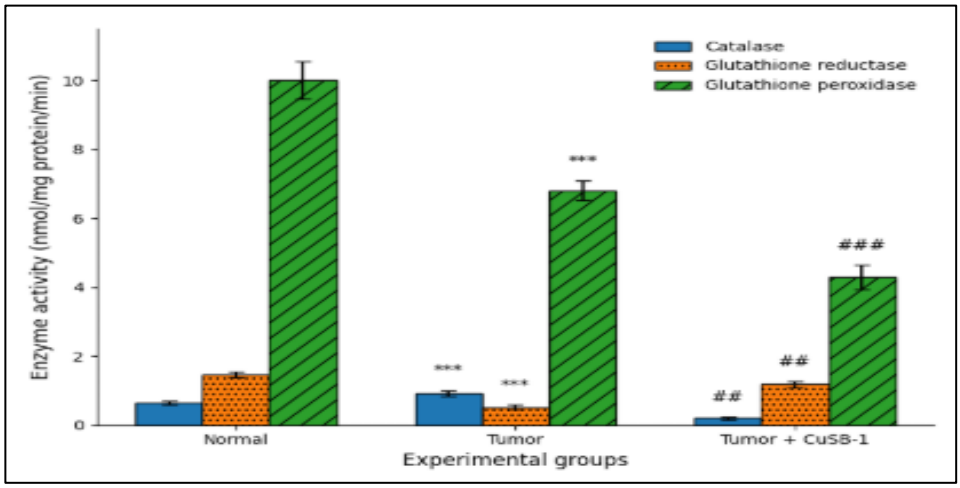

Fig (7): Changes in antioxidant enzyme activities in the breast tumor tissues of different groups treated with CuSB-1 [Cu(phenim)Cl_2]. Values are mean ± S.E.M of four separate experiments. *، ** and * show significant differences at $p < 0.05$، $p < 0.01$ and $p < 0.001$، respectively، when compared with the normal control group (Group I). #، ## and ### indicate statistically significant differences at $p < 0.05$، $p < 0.01$ and $p < 0.001$، respectively، compared to the untreated tumor group (Group II)**

These results suggest that CuSB-1 has a profound effect on the antioxidant system in tumor cells، which may contribute to an increase in oxidative stress-induced cell death.

The FT-IR spectral results provide good evidence for coordination of the phenim Schiff base ligand to the Cu(II) ion in all complexes Cu1-Cu11. The free Schiff base ligand exhibits a typical azomethine (C=N) stretch band at 1625 cm^{-1}، as reported previously [24]. The UV-Visible spectroscopy also confirms the structure and coordination of Cu (II) complexes. The $\pi \rightarrow \pi^*$ transitions (260-290 nm) and $n \rightarrow \pi^*$ transitions (320-360 nm) are common for aromatic Schiff base ligands and azomethine groups، respectively [25]. The ligand-to-metal charge transfer (LMCT) bands in 380-450 nm regions suggest strong metal-ligand interactions، which are important for redox activity and biological activity [26]. The broad and weak d-d bands (600-720 nm) indicate distortion (possibly of Jahn-Teller type) in the octahedral or square pyramidal geometry of Cu (II) (d^9) complexes [27]. It is important to note that LMCT and d-d bands are red shifted in complexes containing strong field ligands (CN^- and SCN^-) suggesting strong ligand-metal interactions، and therefore، greater stability of the metal. This is in line with ligand field theory where high field ligands cause larger crystal field splitting and therefore، larger effect on electronic transitions [28]. Synthesis and purity of the complexes were also verified by elemental (CHN) analysis. The calculated and found values (deviations < ±0.4%) indicate the stoichiometry is correct and there are minimal impurities. These deviations are probably caused by experimental error or traces of solvent، but are acceptable for metal complexes [29].

The cytotoxicity results indicate the prepared copper (II) Schiff base complexes exhibit varying antiproliferative activities، which depend on the nature of the ligands. CuSB-1 [Cu (phenim)Cl_2] is the most active complex with IC_{50} values in the low micromolar range for the three cell lines (MCF-7، PC3 and HEK-293). This increased potency is probably a result of the optimal coordination geometry of the tridentate ligand (phenim)، stabilising the Cu(II) ion while also maintaining flexibility for biological interactions. The lower activity of the free ligand (phenim) and copper salt ($CuCl_2$) suggests that the complex is necessary for activity، suggesting a possible synergy between the metal and the ligand. This is consistent with previous reports in which the metal ion enhances the lipophilicity، enhancing the absorption into the cells and interaction with biological targets (DNA and proteins) [11،30]. Moreover، the variation in IC_{50} values of complexes Cu1-Cu11 indicates that the monodentate ligands play a role in modulating the activity. In particular، complexes with better donor ligands (e.g.، CN^-، SCN^-) were more active than complexes with weaker donor ligands، presumably as a result of more ligand field stabilization and modification of the metal potentials [3]. These effects influence the ability of the complex to undergo redox cycling and to generate reactive oxygen species (ROS) that will cause oxidative stress and cell death in cancer cells [31]. CuSB-1 was found to be more active than Cisplatin in vitro. This may be due to the different mode of action of copper complexes، which is not only due to DNA binding but also involves the redox damage، proteasome and mitochondrial damage، while cisplatin mainly causes DNA crosslinks [32،33]. The DNA binding data is also consistent with the cytotoxicity data. The decrease in fluorescence of the EB-DNA complex in the presence of CuSB-1 indicates CuSB-1 disrupts the EB-DNA complex suggesting that it does bind strongly to DNA. The absence of quenching in control experiments (no DNA or EB، or free ligand and $CuCl_2$) indicates that the quenching is indeed due to the Cu(II) complex. The Stern-Volmer quenching constant (KSV = 0.28) indicates moderate binding، which is consistent with non-covalent binding (intercalation or groove binding). The aromaticity of the phenim ligand can facilitate π-stacking with the DNA bases، while the Cu (II) metal centre can increase the binding through electrostatic interactions with the anionic phosphate backbone of DNA [34]. Moreover، the relatively low KSV value suggests optimal binding strength and reversibility، which is important for anticancer drugs since excessive binding can lead to non-specific toxicity [35].

The displacement of EB also supports the idea that CuSB-1 displaces EB and may therefore be an intercalator which may lead to DNA cleavage، as has been seen for other copper (II) Schiff bases [36،20]. In vivo studies demonstrate the better anti-tumor effect of CuSB-1 ([Cu (phenim) Cl_2]) compared to conventional chemotherapy. The high tumor volume suppression (55%) and decrease in the specific growth rate in CuSB-1-treated mice indicates that the complex effectively prevents tumor growth. In contrast، Cisplatin showed weak antitumor effect (22%) revealing the enhanced effect of the copper complex. This enhanced antitumor activity can be attributed to the redox activity of Cu (II) that enables the complex to undergo intracellular redox cycling that leads to the production of reactive oxygen species (ROS). The increased ROS levels cause oxidative stress، resulting in DNA، protein and lipid damage، and induce apoptosis in cancer cells [37]. Unlike cisplatin، which has a single target (DNA crosslinking), copper complexes such as CuSB-1 display a multi-faceted mechanism of action، including oxidative stress، mitochondrial targeting، and survival pathway blockade [38]. The doubling time of tumors is also increased (~2-fold)، suggesting an antiproliferative effect of CuSB-1. This would mean that CuSB-1 kills tumour cells and also blocks cell growth. This is probably due to the interference with regulatory processes such as the Akt pathway and

cell cycle checkpoints، which are often altered in cancer [39]. This weight control experiment also indicates the effectiveness of CuSB-1. The body weight of tumor bearing mice was significantly enhanced، but this was reversed by CuSB-1. Importantly، the absence of significant weight loss points to low systemic toxicity، a major side effect of cisplatin therapy. This could be due to the selective redox activity of the copper complex in cancer cells، which are under higher oxidative stress [40].

The histopathological investigations also support the activity of CuSB-1. The large number of apoptotic bodies and chromatin condensation seen in the tumors indicate the induction of high levels of apoptosis، whereas the control tumors show a dense growth of carcinoma cells. In contrast، only a low number of apoptotic bodies were observed in the cisplatin-treated tissues without the presence of chromatin condensation، suggesting that it is not as effective as an inducer of apoptosis. These observations are consistent with previous work that copper complexes were found to induce apoptosis via both intrinsic (mitochondrial) and extrinsic pathways [41]. The mitotic index and the apoptotic index provide strong evidence for the mode of action. The mitotic index of CuSB-1 was found to be dramatically reduced and the apoptotic index dramatically increased، which is an indication of a shift from growth to death. This is important in cancer treatment as it may lead to a reduction of tumor growth and death of cancer cells. The elevated apoptotic index in CuSB-1 compared to cisplatin may be due to the induction of the apoptotic pathway، which may have occurred via activation of caspases and other pro- or anti-apoptotic proteins such as Bax and Bcl-2 [42]. The decrease in the activity of the antioxidant enzymes in the tumor following CuSB-1 treatment suggests a disruption of the antioxidant system. Catalase and GPx play a crucial role in the degradation of reactive oxygen species (ROS) (hydrogen peroxide and lipid peroxides، respectively) and in the maintenance of the redox status [43]. The 5-fold reduction in the activity of catalase indicates a significant reduction in the metabolism of hydrogen peroxide in tumor cells. This can result in increased oxidative stress and damage to macromolecules (DNA، proteins and lipids). By contrast، the increased glutathione reductase (GR) activity in CuSB-1-treated tissues (~2-fold) could be a response to the oxidative stress. This enzyme is able to convert the oxidized glutathione (GSSG) into reduced glutathione (GSH) to attempt to restore the glutathione redox balance [44]. But، although the activity of GR is higher، the antioxidant system is impaired due to the lower activity of catalase and GPx. This results in an increase in the total ROS level، and therefore، apoptosis. CuSB-1 has a selective effect on antioxidant systems as a result of the redox capability of Cu (II). Cu (II) complexes are capable of Fenton reactions (Cu(II) to Cu(I) or vice versa) and production of ROS. This becomes even more effective in cancer cells as they are in a state of oxidative stress، so are more vulnerable to ROS attack [35]. Thus، CuSB-1 takes advantage of this by overriding the antioxidant response of the cells and hence، causes oxidative stress and cell death. The biochemical results are in line with the histopathological and apoptotic changes described above، which revealed an increase in apoptosis and reduction in proliferation. This has been shown to lead to mitochondrial dysfunction، the release of cytochrome c and subsequent caspase activation and apoptosis [45].

4- CONCLUSION

This study synthesized and characterized copper (II) Schiff base complexes of phenim and the most active compound was CuSB-1 [Cu(phenim)Cl_2]. CuSB-1 was found to have good in vitro cytotoxicity and DNA binding، which implies potential interactions with biomolecules. The in vivo experiments showed good tumor growth inhibition، apoptosis، and better antitumor activity than Cisplatin. CuSB-1 acts via the modulation of the antioxidant system resulting in cell death through the ROS-mediated pathway. In conclusion، CuSB-1 is a potential multi-target cancer drug and hence needs to be investigated further.

REFERENCES

[1] Rosenberg, B., VanCamp, L., Trosko, J. E., and Mansour, V. H. (1969). Platinum compounds: A new class of potent antitumour agents. *Nature*, *222*(5191), 385–386. https://doi.org/10.1038/222385a0

[2] da Silva, D. A., De Luca, A., Squitti, R., Rongioletti, M., Rossi, L., Machado, C. M. L., and Cerchiaro, G. (2022). Copper in tumors and the use of copper-based compounds in cancer treatment. *Journal of Inorganic Biochemistry*, *226*, 111634. https://doi.org/10.1016/j.jinorgbio.2021.111634

[3] Ghosh, S. (2019). Cisplatin: The first metal based anticancer drug. *Bioorganic Chemistry*, *88*, Article 102925. https://doi.org/10.1016/j.bioorg.2019.102925

[4] Dasari, S., and Tchounwou, P. B. (2014). Cisplatin in cancer therapy: Molecular mechanisms of action. *European Journal of Pharmacology*, *740*, 364–378. https://doi.org/10.1016/j.ejphar.2014.07.025

[5] Amable, L. (2016). Cisplatin resistance and opportunities for precision medicine. *Pharmacological Research*, *106*, 27–36. https://doi.org/10.1016/j.phrs.2016.01.001

[6] Blades, B., Ayton, S., Hung, Y. H., Bush, A. I., and La Fontaine, S. (2021). Copper and lipid metabolism: A reciprocal relationship. *Biochimica et Biophysica Acta (BBA) - General Subjects*, *1865*(11), Article 129979. https://doi.org/10.1016/j.bbagen.2021.129979

[7] Afsan, Z., Roisnel, T., Tabassum, S., and Arjmand, F. (2020). Structure elucidation (spectroscopic, single crystal X-ray diffraction and computational DFT studies) of new tailored benzenesulfonamide derived Schiff base copper(II) intercalating complexes: Comprehensive biological profile (DNA binding, pBR322 DNA cleavage, Topo I inhibition and cytotoxic activity). *Bioorganic Chemistry*, *94*, Article 103427. https://doi.org/10.1016/j.bioorg.2019.103427

[8] Kongot, M., Reddy, D., Singh, V., Patel, R., Singhal, N. K., and Kumar, A. (2019). Potent drug candidature of an ONS donor tethered copper (II) complex: Anticancer activity, cytotoxicity and spectroscopically approached BSA binding studies. *Spectrochimica Acta Part A: Molecular and Biomolecular Spectroscopy*, *212*, 330–342. https://doi.org/10.1016/j.saa.2019.01.020

[9] Locke, J. M., Griffith, R., Bailey, T. D., and Crumbie, R. L. (2009). Competition between cyclisation and bisimine formation in the reaction of 1,3-diaminopropanes with aromatic aldehydes. *Tetrahedron*, *65*(51), 10685–10692. https://doi.org/10.1016/j.tet.2009.10.057

[10] Halimehjani, A. Z., Movahed, F. S., Fathi, M. B., Daliri, R., and Saidi, M. R. (2019). Investigation of complexation behavior of the dithiocarbamates of *N*,*N*-dicinnamylalkane-1,*n*-diamines with metals. *Journal of Molecular Structure*, *1180*, 188–195. https://doi.org/10.1016/j.molstruc.2018.11.102

[11] Cerchiaro, G., Aquilano, K., Filomeni, G., Rotilio, G., Ciriolo, M. R., and Ferreira, A. M. D. C. (2005). Isatin-Schiff base copper(II) complexes and their influence on cellular viability. *Journal of Inorganic Biochemistry*, *99*(7), 1433–1440. https://doi.org/10.1016/j.jinorgbio.2005.03.013

[12] Ray, A., Bar, N., Chowdhury, P., Biswas, D., Ghosh, K., Mandi, A., and Das, G. K. (2023). Revaluation of copper(II)-Schiff base complex for sensing of D-penicillamine and development of a molecular logic gate: A combined approach. *Polyhedron*, *243*, Article 116563. https://doi.org/10.1016/j.poly.2023.116563

[13] Mohamed, G. G., and Sharaby, C. M. (2007). Metal complexes of Schiff base derived from sulphametrole and o-vanilin: Synthesis, spectral, thermal characterization and biological activity. *Spectrochimica Acta Part A: Molecular and Biomolecular Spectroscopy*, *66*(4–5), 949–958. https://doi.org/10.1016/j.saa.2006.04.033.

[14] Gowda, N. M. N., Naikar, S. B., and Reddy, G. K. N. (1984). Perchlorate ion complexes. *Advances in Inorganic Chemistry*, *28*, 255–299. https://doi.org/10.1016/S0898-8838(08)60208-6

[15] Lavanant, H., Virelizier, H., and Hoppilliard, Y. (1998). Reduction of copper(II) complexes by electron capture in an electrospray ionization source. *Journal of the American Society for Mass Spectrometry*, *9*(11), 1217–1221. https://doi.org/10.1016/S1044-0305(98)00100-7

[16] Müller, J., Felix, K., Maichle, C., Lengfelder, E., and Weser, U. (1995). Phenyl-substituted copper di-Schiff base, a potent Cu_2Zn_2 superoxide dismutase mimic surviving competitive biochelation. *Inorganica Chimica Acta*, *233*(1–2), 11–19. https://doi.org/10.1016/0020-1693(94)04298-A

[17] Lewandowska, A. M., Lewandowski, T., Rudzki, M., Rudzki, S., and Laskowska, B. (2021). Cancer prevention -review paper. *Annals of Agricultural and Environmental Medicine*, *28*(1), 11–19. https://doi.org/10.26444/aaem/116906

[18] Pilleron, S., Sarfati, D., Janssen-Heijnen, M., Vignat, J., Ferlay, J., Bray, F., and Soerjomataram, I. (2018). Global cancer incidence in older adults, 2012 and 2035: A population-based study. *International Journal of Cancer*, *144*(1), 49–58. https://doi.org/10.1002/ijc.31664

[19] Salehi, M., Faghani, F., Kubicki, M., and Bayat, M. (2018). New complexes of Ni(II) and Cu(II) with tridentate ONO Schiff base ligand: Synthesis, crystal structures, electrochemical and theoretical investigation. *Journal of the Iranian Chemical Society*, *15*(10), 2229–2240. https://doi.org/10.1007/s13738-018-1412-1

[20] Temel, H., Ziyadanoğullari, B., Aydın, I., and Aydın, F. (2005). Synthesis, spectroscopic and thermodynamic studies of new transition metal complexes with *N*,*N*′-bis(2-hydroxynaphthalin-1-carbaldehydene)-1,2-bis(*m*-aminophenoxy)ethane and their determination by spectrophotometric methods. *Journal of Coordination Chemistry*, *58*(14), 1177–1185. https://doi.org/10.1080/00958970500078890

[21] Tümer, M., Akgün, E., Toroğlu, S., Kayraldiz, A., and Dönbak, L. (2008). Synthesis and characterization of Schiff base metal complexes: Antimicrobial, genotoxicity and electrochemical properties. *Journal of Coordination Chemistry*, *61*(18), 2935–2949. https://doi.org/10.1080/00958970802012117

[22] Champouret, Y. D. M., Fawcett, J., Nodes, W. J., Singh, K., and Solan, G. A. (2006). Spacially confined M_2 centers (M = Fe, Co, Ni, Zn) on a sterically bulky binucleating support: Synthesis, structures and ethylene oligomerization studies. *Inorganic Chemistry*, *45*(24), 9890–9900. https://doi.org/10.1021/ic061286x

[23] Liu, X., Manzur, C., Novoa, N., Celedón, S., Carrillo, D., and Hamon, J. R. (2018). Multidentate unsymmetrical Schiff bases and their metal complexes: Synthesis, properties and catalytic applications. *Coordination Chemistry Reviews*, *357*, 144–172. https://doi.org/10.1016/j.ccr.2017.11.030

[24] Caviglia, M., Li, Z., Santini, C., Del Gobbo, J., Cimarelli, C., Du, M., Dolmella, A., & Pellei, M. (2025). New Cu(II), Cu(I) and Ag(I) Complexes of Phenoxy-Ketimine Schiff Base Ligands: Synthesis, Structures and Antibacterial Activity. *Molecules*, *30*(9), 1893. https://doi.org/10.3390/molecules30091893

[25] Kawamoto, T., Nishiwaki, M., Tsunekawa, Y., Nozaki, K., and Konno, T. (2008). Synthesis and characterization of luminescent zinc(II) and cadmium(II) complexes with N,S-chelating Schiff base ligands. *Inorganic Chemistry*, *47*(8), 3095–3104. https://doi.org/10.1021/ic7020758

[26] Yousif, E., Majeed, A., Al-Sammarrae, K., Salih, N., Salimon, J., and Abdullah, B. (2017). Metal complexes of Schiff base: Preparation, characterization and antibacterial activity. *Arabian Journal of Chemistry*, *10*, S1639–S1644. https://doi.org/10.1016/j.arabjc.2013.06.006

[27] Al Zoubi, W., Al-Hamdani, A. A. S., Ahmed, S. D., & Ko, Y. G. (2018). Synthesis, characterization and biological activity of Schiff base metal complexes. *Journal of Physical Organic Chemistry*, *31*(1), e3752. https://doi.org/10.1002/poc.3752

[28] Iftikhar, B., Javed, K., Khan, M. S. U., Akhter, Z., Mirza, B., & McKee, V. (2018). Synthesis and biological evaluation of salicylaldehyde Schiff base Cu(II) complexes. *Journal of Molecular Structure*, *1155*, 337–348. https://doi.org/10.1016/j.molstruc.2017.11.002

[29] Tadavi, S. K., Yadav, A. A., & Bendre, R. S. (2018). Synthesis and characterization of Schiff base complexes with biological activity. *Journal of Molecular Structure*, *1152*, 223–231. https://doi.org/10.1016/j.molstruc.2017.09.088

[30] Malik, M. A., Dar, O. A., Gull, P., Wani, M. Y., & Hashmi, A. A. (2018). Schiff base transition metal complexes in antimicrobial and anticancer therapy. *MedChemComm*, *9*(3), 409–436. https://doi.org/10.1039/C7MD00526A

[31] Andiappan, K., Sanmugam, A., Deivanayagam, E., Karuppasamy, K., Kim, H. S., & Vikraman, D. (2018). Cytotoxic activity of Schiff base lanthanide complexes. *Scientific Reports*, *8*(1), 3054. https://doi.org/10.1038/s41598-018-21366-0

[32] Palanimurugan, A., & Kulandaisamy, A. (2018). DNA interaction and anticancer activity of Schiff base metal complexes. *Journal of Organometallic Chemistry*, *861*, 263–274. https://doi.org/10.1016/j.jorganchem.2018.02.043

[33] Oladipo, S. D., Omondi, B., & Mocktar, C. (2020). Co(III) N,N′-diarylformamidine dithiocarbamate complexes: Synthesis, characterization, crystal structures and biological studies. *Applied Organometallic Chemistry*, *34*(4), e5610. https://doi.org/10.1002/aoc.5610

[34] Oladipo, S. D., Mocktar, C., & Omondi, B. (2020). In vitro biological studies of heteroleptic Ag(I) and Cu(I) unsymmetrical N,N′-diarylformamidine dithiocarbamate phosphine complexes: Effect of the metal center. *Arabian Journal of Chemistry*, *13*(7), 6379–6394. https://doi.org/10.1016/j.arabjc.2020.05.034

[35] Ndagi, U., Lawal, M. M., & Soliman, M. E. (2019). DFT study of structural and electronic properties of organogold(III) compounds with anticancer activity. *Russian Journal of Physical Chemistry A*, *93*(8), 1543–1558. https://doi.org/10.1134/S003602441908020X

[36] Lawal, M. M., Lawal, I. A., Klink, M. J., Tolufashe, G. F., Ndagi, U., & Kumalo, H. M. (2020). Density functional theory study of gold(III)-dithiocarbamate complexes with anticancer potential. *Journal of Inorganic Biochemistry*, *206*, 111044. https://doi.org/10.1016/j.jinorgbio.2020.111044

[37] Galvan, M., Vela, A., & Gázquez, J. L. (1988). Chemical reactivity in spin-polarized density functional theory. *The Journal of Physical Chemistry*, *92*(23), 6470–6474. https://doi.org/10.1021/j100334a008

[38] Ugbaja, S. C., Sanusi, Z. K., Appiah-Kubi, P., Lawal, M. M., & Kumalo, H. M. (2021). Computational modelling of β-secretase (BACE1) inhibitors for Alzheimer's disease. *Biophysical Chemistry*, *270*, 106536. https://doi.org/10.1016/j.bpc.2020.106536

[39] Magwenyane, A. M., Mhlongo, N. N., Lawal, M. M., Amoako, D. G., Somboro, A. M., Sosibo, S. C., Kumalo, H. M., & Soliman, M. E. (2020). Structural insights into Hsp90 inhibitors: Dynamics and therapeutic activity. *Molecules*, *25*(8), 1785. https://doi.org/10.3390/molecules25081785

[40] Ejalonibu, M. A., Elrashedy, A. A., Lawal, M. M., Soliman, M. E., Sosibo, S. C., Kumalo, H. M., & Mhlongo, N. N. (2020). Dual targeting approach for Mycobacterium tuberculosis drug discovery: DFT and molecular dynamics insights. *Structural Chemistry*, *31*(2), 557–571. https://doi.org/10.1007/s11224-019-01429-1

[41] Akinpelu, O. I., Lawal, M. M., Kumalo, H. M., & Mhlongo, N. N. (2020). Computational study of trisubstituted benzimidazoles as antitubercular agents. *Journal of Biomolecular Structure and Dynamics*, *39*(14), 5122–5134. https://doi.org/10.1080/07391102.2020.1784793

[42] Akinpelu, O. I., Lawal, M. M., Kumalo, H. M., & Mhlongo, N. N. (2020). Drug repurposing of fusidic acid as inhibitor of *Mycobacterium tuberculosis* FtsZ polymerization. *Tuberculosis*, *121*, 101920. https://doi.org/10.1016/j.tube.2020.101920

[43] Adeowo, F. Y., Ejalonibu, M. A., Elrashedy, A. A., Lawal, M. M., & Kumalo, H. M. (2020). Multi-target approach for Alzheimer's disease: Modeling of cholinesterase enzymes with quinoline derivatives. *Journal of Biomolecular Structure and Dynamics*, *39*(16), 6140–6156. https://doi.org/10.1080/07391102.2020.1798814

[44] Ibeji, C. U., Lawal, M. M., Tolufashe, G. F., Govender, T., Naicker, T., Maguire, G. E., & Soliman, M. E. (2019). QM/MM study of β-lactam antibiotic acylation by L, D-transpeptidase 2. *ChemPhysChem*, *20*(9), 1126–1134. https://doi.org/10.1002/cphc.201900135

[45] Sun, X., Tang, S., Hou, B., Duan, Z., Liu, Z., Li, Y., He, S., Wang, Q., & Chang, Q. (2021). Overexpression of P-glycoprotein, MRP2 and CYP3A4 impairs intestinal absorption of octreotide in rats with portal hypertension. *BMC Gastroenterology*, *21*(1), 2. https://doi.org/10.1186/s12876-020-01582-7